Shahrood University of Technology

Journal of Mining and Environment (JME)

Journal homepage: www.jme.shahroodut.ac.ir

Iranian Society of Mining Engineering (IRSME)

Automatic Identification of Salt Dome Geobody in 2D Seismic Data using Metaheuristic-based Clustering of Textural Attributes

Poorandokht Soltani[1], Amin Roshandel Kahoo[1*], and Hamid Hassanpour[2]

1. Faculty of Mining, Petroleum and Geophysics Engineering, Shahrood University of Technology, Shahrood, Iran
2. Faculty of Computer Engineering, Shahrood University of Technology , Shahrood, Iran

Article Info

Received 9 July 2025
Received in Revised form 21 October 2025
Accepted 30 December 2025
Published online 30 December 2025

DOI: 10.22044/jme.2025.16491.3224

Keywords

Seismic attributes
Texture analysis
Attribute selection
Clustering
Metaheuristic Optimization

Abstract

Seismic methods are among the primary and most effective techniques for hydrocarbon exploration, as they enable comprehensive imaging and interpretation of the Earth's subsurface. However, accurate interpretation of seismic data requires detailed analysis of geological structures, often involving complex and subjective decision-making processes. Constructing an initial geological model that aligns with seismic observations is a critical first step, but it is inherently non-unique and heavily influenced by the interpreter's experience and preferences. Among various subsurface structures, salt domes are of particular interest due to their unique physical characteristics and their critical role in hydrocarbon entrapment, drilling risk management, and subsurface storage applications. Their distinct seismic textures, compared to surrounding sediments, make them identifiable using seismic texture attributes. Nevertheless, the manual delineation of salt dome geobody is a time-consuming and potentially error-prone task, especially given the volume, redundancy, and complexity of the seismic attributes used. To overcome these challenges, we propose a novel unsupervised framework for automatically identifying salt dome geobody in 2D seismic sections. The method begins by extracting a diverse set of seismic texture attributes, including both conventional attributes and novel texture descriptors derived from advanced image analysis techniques. Following attribute extraction, a attribute selection phase using techniques such as Laplacian Score is employed to eliminate redundant, irrelevant, or highly correlated attributes, thereby enhancing model efficiency and interpretability. The reduced set of relevant attributes is then used as input for clustering algorithms based on metaheuristic optimization techniques. These algorithms aim to partition the seismic data into meaningful clusters that correspond to geological attributes, particularly salt domes. Validation against multiple expert interpretations demonstrates the robustness and high accuracy of the proposed method. Results emphasize the capability of unsupervised clustering approaches especially those guided by metaheuristic strategies—in reducing interpretation uncertainty and improving segmentation quality.

1. Introduction

Understanding subsurface geological structures is a fundamental aspect of energy resource exploration, particularly in identifying potential oil and gas reserves. Seismic interpretation, the cornerstone of hydrocarbon exploration, relies on analyzing subsurface pseudo-images generated through seismic reflection [9]. However, manual interpretation of

Corresponding author: roshandel@shahroodut.ac.ir (A. Roshandel Kahoo)

seismic sections is inherently uncertain, subjective, and time-consuming, often requiring expert judgment [28]. This has driven the advancement of quantitative seismic interpretation, where seismic attributes play a pivotal role in revealing subtle geological features and facilitating automated analysis [23; 29]. Seismic attributes are quantitative measures derived from seismic data that reflect geological, geophysical, or mathematical properties of the subsurface [47]. The use of seismic attributes began in the 1950s, but the digitalization of seismic data in the 1960s catalyzed the development of more sophisticated processing techniques. The 1980s marked a surge in attribute-based interpretation, particularly with the advent of 3D seismic surveys and texture analysis [12]. By the 1990s, seismic attributes had become indispensable for structural and stratigraphic interpretation. Researchers such as Meldahl et al. [43], Roberts [45], and Cohen et al. [13] introduced discontinuity, curvature, and entropy attributes to enhance fault and structural detection.

Among the various categories of seismic attributes, textural attributes have become essential for analyzing seismic image patterns. These attributes quantify spatial variations in amplitude, treating seismic sections as images composed of distinguishable textural patches [8]. In seismology, texture is defined as the spatial variation in seismic amplitude, equivalent to the distribution of intensity values in a digital image [12]. Various approaches have been developed for texture analysis, which can be broadly categorized into statistical, structural, transform-based, model-based, graph-based, learning-based, and entropy-based methods [31]. Statistical methods, particularly those based on the gray-level co-occurrence matrix [25], are the most widely used due to their efficiency in capturing spatial relationships.

Among the geological structures detectable through textural attributes, salt domes are particularly important. These diapiric formations rise through overlying sedimentary layers because of their lower density. Accurate delineation of salt domes is essential, as they significantly influence hydrocarbon trap formation, underground storage potential, and drilling safety [24]. In seismic sections, salt domes display unique textures resulting from their distinct petrophysical and elastic properties, making them prominent targets for texture-based interpretation [34; 46; 50]. The GLCM-based approach is a prominent technique for detecting salt domes. Eichkitz et al. [19] extended this method to 3D seismic volumes, enabling more accurate delineation. To improve performance, Di et al. [16] proposed non-linear rescaling of seismic data before GLCM calculation. Moreover, many studies have combined GLCM attributes with supervised learning, clustering, and data fusion techniques to enhance geobody detection [4; 59]. Nonetheless, traditional texture descriptors such as GLCM are limited in capturing complex geological attributes and are often sensitive to the orientation of seismic events.

To address the limitations of classical methods, alternative approaches have been developed. These include gradient-based attributes [20], Sobel edge detection [3], and texture extraction using Fourier and Gabor transforms [52]. Additionally, the Histogram of Oriented Gradients, a widely used technique in image processing, has been adapted for seismic data analysis. Hosseini-Fard et al. [29] and Khayer et al. [34] introduced novel HOG-based attributes and fusion frameworks for salt dome segmentation. Another notable innovation is the SalSi attribute, developed by Shafiq et al. [50], which uses saliency-based theory to highlight geobodies in seismic volumes by modeling human visual perception.

With the emergence of machine learning, multi-attribute analysis—integrating both traditional and modern texture attributes—has become increasingly important for reducing interpretation uncertainty. Supervised approaches, particularly convolutional neural networks (CNNs), have been successfully employed for automated interpretation of faults [35], salt domes [17; 55], and seismic facies [60]. Additional advancements include dimensionality reduction methods such as UMAP and clustering frameworks like AMFAA, which improve resolution and interpretational accuracy. For example, Liu et al. [39] and Wang et al. [56] reported up to a 16% improvement in seismic facies prediction in turbidite reservoirs in China. Amin and Deriche [4]; Amin et al. [5] introduced

dictionary-based codebook classification, which outperformed earlier techniques in salt dome detection. While supervised learning offers high predictive power, it is heavily reliant on extensive labeled datasets, which are difficult to obtain in geologically complex environments. Unsupervised learning has gained traction as a viable alternative to supervised methods, particularly due to its independence from labeled training data. Mammadov et al. [42] proposed an efficient unsupervised clustering algorithm for seismic facies that reduced human bias and improved classification precision. Seydoux et al. [49] applied deep scattering networks and clustering to uncover continuous patterns in seismic data. Yang et al. [57] and Naseer [44] also emphasized the value of unsupervised, automated multi-attribute analysis. Graph-based clustering frameworks [33], deep clustering models [9], and unsupervised detection tools [18] represent promising steps toward scalable, automated seismic interpretation. Despite their promise, unsupervised techniques are often sensitive to the selection of input attributes and algorithmic parameters.

This study aims to automatically and unsupervisedly delineate salt dome geobodies in 2D seismic data by clustering textural seismic attributes using a metaheuristic optimization approach. Unlike traditional clustering methods such as k-means-which often struggle with overlapping cluster boundaries-our method employs metaheuristic algorithms to dynamically determine the optimal number of clusters. This approach enhances interpretational robustness while eliminating the need for labeled training data. By combining conventional and novel texture-based seismic attributes, the proposed method improves clustering resolution and addresses the limitations of both manual interpretation and classical machine learning models. Unlike most previous studies that rely either on supervised learning or on classical clustering with fixed parameters, our approach integrates adaptive attribute selection with metaheuristic-driven clustering, providing a fully unsupervised and data-driven framework for salt dome detection.

2. Methodology

In this study, an unsupervised approach is proposed for the automatic detection of salt domes in two-dimensional seismic data, thereby eliminating the need for labeled training datasets. The method begins with the extraction of seismic attributes from pre-processed seismic sections. These attributes include various texture-based seismic indicators, encompassing both conventional and newly developed attributes that are particularly sensitive to reflection patterns associated with salt dome structures.

To mitigate the impact of random noise on clustering outcomes, an initial segmentation is applied to the seismic section, resulting in the generation of super-pixels. Each super-pixel is assigned a representative value, calculated as the average of the pixel values contained within it. This super-pixelization process is uniformly applied across all extracted seismic attributes.

To enhance classification accuracy and remove redundant or irrelevant information, an attribute selection strategy based on the Laplacian Score method is employed. This technique identifies a subset of the most informative super-pixeled seismic attributes, which are then used for the subsequent clustering process.

The separation of salt dome structures from the surrounding stratigraphy is achieved through a meta-heuristic optimization algorithm. The clustering algorithm is specifically designed to capture complex, non-linear patterns in high-dimensional data.

Finally, the performance and accuracy of the proposed method are evaluated through comparison with manually interpreted salt dome boundaries, annotated by multiple expert interpreters. The complete workflow of the proposed approach is illustrated in the flowchart presented in Figure 1. The following sections provide a detailed explanation of each phase of the methodology.

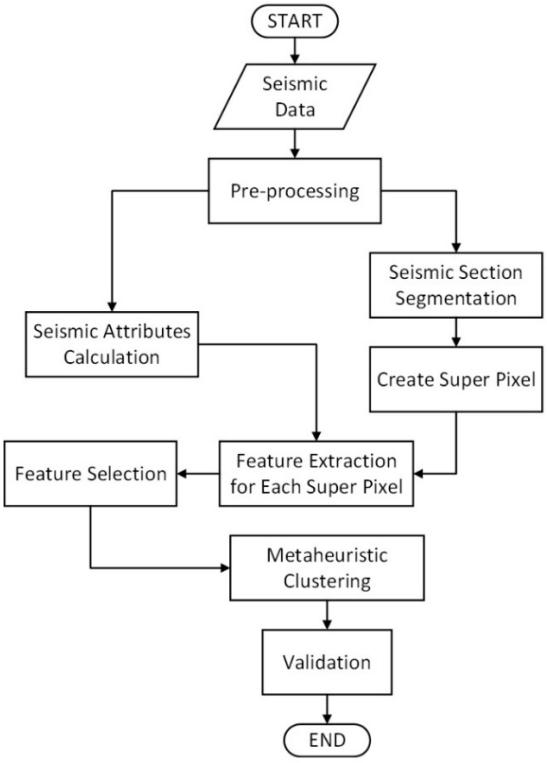

Figure 1. The complete workflow of the proposed approach [54].

2.1. Pre-processing data

The seismic data used in this study is part of a 2D seismic section that includes a salt dome. These post-stack, time-migrated data consist of 1,000-time samples and approximately 700 spatial samples, acquired with a sampling interval of 4 milliseconds.

The computation of seismic attributes is carried out in two main steps. In the first step, the seismic data is converted into a grayscale image. This involves mapping the amplitude values from the range $[a_{min}, a_{max}]$ to the grayscale range $[0, N_g - 1]$, where a_{min} و a_{max} are the minimum and maximum amplitudes of the seismic signal, and N_g represents the number of grayscale levels. The most basic and widely used approach for this conversion is linear transform, which preserves the histogram of the original amplitude distribution and maintains the overall appearance of the seismic section. However, in many cases, the attributes of interest occupy only a small portion of the full amplitude range. Therefore, allocating more grayscale levels to this range can enhance their visibility in the grayscale image. To achieve this, non-linear transform functions-such as logarithmic, exponential, logistic, and particularly the sigmoid function-can be employed. The sigmoid function emphasizes mid-range (weak) amplitudes and compresses the high-amplitude values, resulting in improved visual clarity for subtle attributes. Traditionally, the simplest and most accessible method for rescaling the amplitude of the input image to grayscale is linear transform, which is calculated according to Equation (1).

$$g_l = (a - a_{min}) \frac{N_g - 1}{a_{max} - a_{min}} \quad (1)$$

In this transform, based on the chosen number of grayscale levels N_g, the amplitude range $[a_{min}, a_{max}]$ is divided into N_g equal subranges. Each subrange is then assigned a grayscale level, establishing a linear relationship between seismic amplitudes and their corresponding grayscale levels. This linear mapping preserves the original amplitude histogram to a large extent. To enhance the visibility of specific amplitude ranges, a non-linear transform such as the sigmoid function may be used. The sigmoid-based grayscale value is calculated using Equation (2). Where a is a coefficient that determines the slope of the sigmoid function [15].

$$g_s = \frac{N_g - 1}{1 + \exp\left(-a\left(g_l - \frac{N_g}{2}\right)\right)} \quad (2)$$

In this study, a sigmoid transformation with 32 grayscale levels is used, which provides a good balance between visual resolution and computational efficiency. For attribute extraction, a moving local window is applied over the seismic data. The statistical attribute computed within each window is assigned to its center. The window size must be chosen carefully to be sensitive to the structural variations of interest and should not be smaller than the dominant wavelength of the seismic wavelet [19]. The green line in Figure 8a is the interpreted boundary of the salt dome resulting from the average manual interpretation of three professional interpreters. For textural analysis, this data has been rescaled to grayscale using a nonlinear transform (sigmoid function), which is shown in Figure 8b.

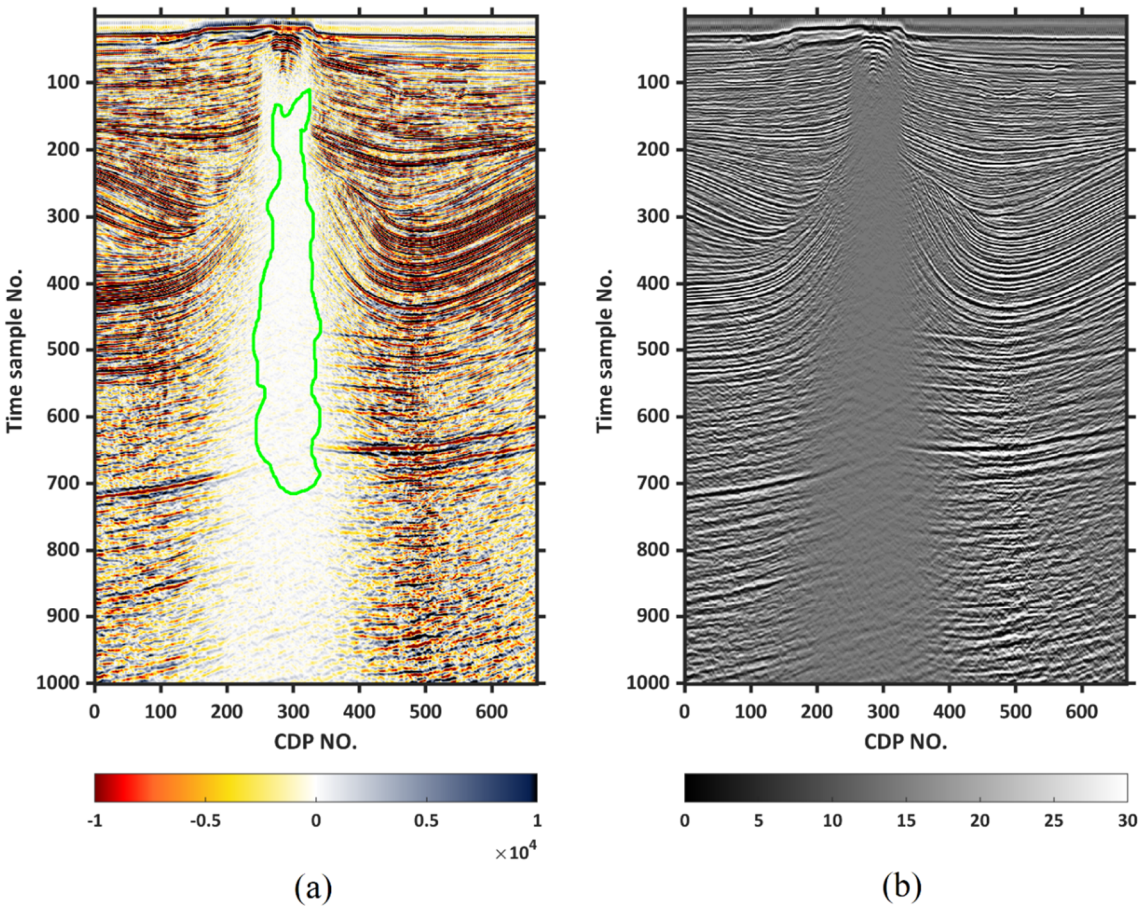

Figure 2. (a) The seismic section from one of the oil fields in the southwest of Iran , and it's rescaled to grayscale by (b) non-linear transform. The green line is the interpreted boundary of the salt dome resulting from the average manual interpretation of three professional interpreters.

2.2. Seismic texture Attributes

Seismic texture attributes represent information derived from seismic data, obtained either through direct measurement or inferred using empirical or logical approaches [11]. Over time, a wide range of seismic attributes have been developed, each tailored to detect specific geological attributes within seismic datasets. To effectively identify and differentiate salt domes, attributes that are sensitive to texture variations can be particularly useful. These texture attributes are commonly generated using image texture analysis techniques and contribute significantly to the enhanced interpretation of seismic sections [31]. In this study, a total of 63 different texture-based seismic texture attributes have been applied, with a brief summary provided in Table 1.

2.3. Super-pixel

For interpreting and clustering seismic sections, a pointwise approach may be utilized, where each data point in the seismic volume is considered an individual sample. These samples are described using various seismic attributes. However, clusters generated using this approach often appear noisy. This is primarily due to inherent seismic data characteristics and numerous factors that introduce errors into the clustering process, such as random noise. As a result, cluster assignments tend to fluctuate over short spatial ranges, producing unstable groupings that may also be affected by the frequency content of the data. Such behavior is generally unsuitable for reliable seismic interpretation. Therefore, the effectiveness of the pointwise method is considered limited, prompting the use of superpixel segmentation

techniques as a more accurate alternative for seismic data analysis [9]. A superpixel is defined as a group of adjacent pixels that are grouped together based on shared characteristics, making them a coherent and meaningful unit in image analysis. Superpixels aid in identifying object positions and boundaries by assigning labels to all pixels in a way that ensures those with the same label share attributes such as color, intensity, or texture. The resulting segments collectively reconstruct the image while ensuring distinct boundaries between adjacent regions based on these attributes.

Table 1. The list of 63 different attributes has been used in this paper.

	Seismic textural attribute	Brief description
Statical approach	Chaos	Statistical methods analyze the spatial distribution of gray levels in seismic texture data to extract meaningful attributes. These methods, describe patterns of intensity variations. They are particularly effective for capturing local structures and subtle textural differences in seismic images [19; 20; 27; 29; 38; 51; 53].
	variance	
	Tamir (Edge contents, directionality, Smoothness)	
	Gradient of texture 2D	
	Gray Level Co-occurrence Matrix (Homogeneity, energy, entropy, trace, Cluster prominence, Correlation)	
	Gray Level Run Length Matrix (Gray-Level Nonuniformity, High Gray-Level Run Emphasis, Low Gray-Level Run Emphasis, Long Run High Gray-Level Emphasis, Run Length Nonuniformity, Short Run High Gray-Level Emphasis)	
	Gray Level Difference Matrix (Angular, entropy, Expectation)	
	Gray Level Size Zone Matrix (Gray-Level Nonuniformity Normalized, Gray-Level Variance, Large Zone Emphasis, Large Zone High Gray-Level Emphasis, Small Zone Emphasis, Small Zone High Gray-Level Emphasis, Zone Entropy, Zone Percentage, Zone-Size Nonuniformity, Zone-Size Nonuniformity, Zone-Size Variance)	
	Neighboring Gray Level Dependence Matrix (Dependence count energy, dependence Entropy , Depended Nonuniformity, Depended Nonuniformity Normalized, dependence Variance , Gray-Level Nonuniformity, Gray-Level Nonuniformity Normalized, gray level Nonuniformity , gray level Nonuniformity Normalized, Large Dependence Emphasis, Large dependence High Gray-Level Emphasis, Small Dependence Emphasis, Small dependence high, Gray-Level Emphasis)	
	Histogram oriented gradient (minimum, Product)	
	Local binary pattern	
Transform approach	Fourier Gabor 0º, 45º, 90º)	It analyzes seismic textures in alternative domains, such as frequency or scale space, by applying mathematical transforms. These methods decompose the seismic image into components at various frequencies and orientations, enabling multi-resolution analysis. They are especially effective for identifying periodic structures, directional patterns, and scale-dependent attributes, which are valuable in characterizing complex geological structures [41; 58].
	Fourier2D (Anisotropy, Regularity, skewness, Kurtosis, average, median)	
Graph based approach	Short path (average, Standard Deviation)	It models the seismic image as a network where pixels or regions are treated as nodes and their relationships form the edges. By analyzing graph properties like node degree, connectivity, and edge weights, meaningful texture attributes can be extracted. These methods are effective in capturing both local and global structural patterns [21; 32].
Entropy based approach	Dispersion	It quantifies the complexity or randomness of gray-level distributions within seismic images. By measuring the uncertainty or disorder in pixel intensity patterns, these approaches can highlight textural irregularities that may correspond to geological attributes. Higher entropy values often indicate more complex textures, while lower values suggest homogeneity. These methods are particularly useful for detecting subtle variations in seismic data that might not be evident through traditional amplitude-based analysis [6; 7; 37].
	Distribution	

Several approaches exist for performing superpixel segmentation in seismic imaging, including algorithms like simple linear iterative clustering [2; 30]. In this study, we employed the adaptive morphological reconstruction (AMR) method to achieve superpixel segmentation.

AMR aims to improve segmentation quality by eliminating insignificant regional minima in gradient images while preserving important edges, which is crucial for accurate segmentation in images with complex textures and noise [36]. Compared to other similar methods, AMR offers significant advantages when applied prior to image clustering. AMR is a morphology-based technique that enhances important structural features while suppressing small-scale noise and irrelevant details. Unlike conventional filtering or preprocessing approaches, AMR adapts locally to the content of the image, preserving essential structures and object boundaries. This preprocessing step ensures that the extracted features for clustering—such as intensity, color, or texture—more accurately represent the true content of the image rather than being distorted by noise or minor artifacts. Consequently, the clustering results become more stable, meaningful, and reflective of the actual image structures, outperforming other methods that do not incorporate adaptive structural reconstruction.

Additionally, we applied the superpixel function to further refine the superpixel segmentation process. This method efficiently partitions the image into compact, uniform regions, promoting better spatial coherence and boundary adherence in segmented outputs. By using the superpixel function, the segmentation achieves high accuracy and is well-suited for handling noisy and structurally intricate seismic images [48].

Figure 3 presents the result of the superpixel segmentation applied to seismic data. In the next stage, to support the clustering process based on superpixel, an attribute vector is calculated for each segment. This attribute vector is computed by averaging the attribute values of all pixels within each superpixel, thereby providing a representative descriptor for clustering.

2.4. Feature Selection

In unsupervised learning tasks such as clustering, the choice of attributes significantly influences the clarity of patterns, computational speed, interpretability, and the ability to generalize. Specifically, in seismic data analysis-where clustering is used to uncover reflection patterns—identifying the most meaningful seismic attributes is a critical step. One effective technique for this purpose is the Laplacian Score, which is advantageous because it does not require labeled data [3]. This method evaluates each attribute based on how well it maintains local similarity structures within the dataset. The core idea is to model the dataset as a graph where each data point is a node (see Appendix A).

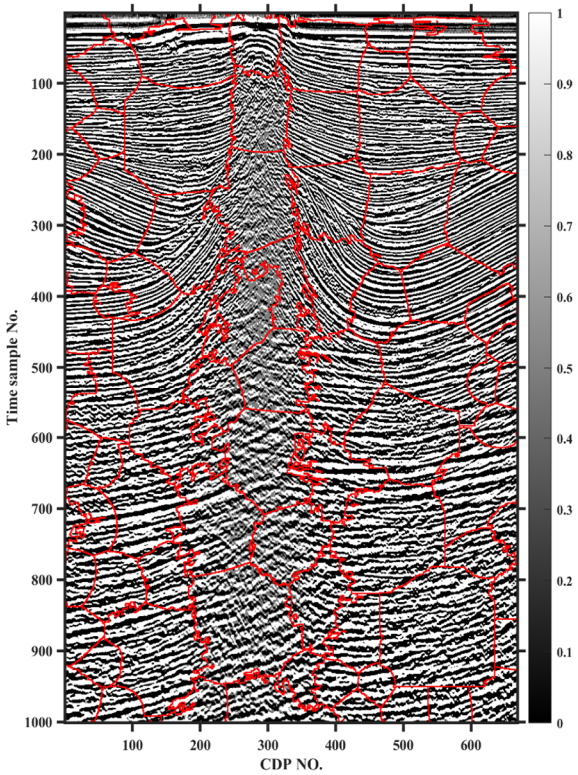

Figure 3. The result of super-pixel segmentation of seismic section.

Since attributes may have different scales, normalization is applied beforehand. Typically, attribute values are rescaled into a [0,1] range to ensure uniform contribution and prevent dominance by attributes with larger numeric ranges. The Laplacian Score was selected because it preserves the local manifold structure of the data, allowing the selection of features that best maintain neighborhood consistency. This property is particularly beneficial in seismic data, where reflection continuity and spatial coherence are key geological attributes.

To decide which attributes to retain, a ranking plot is analyzed-similar in spirit to the elbow method. Instead of setting a fixed threshold, the

method examines visible changes in the ranking slope to select the most impactful attributes. As illustrated in Figure 5, 21 attributes were finally selected. These accounted for over 50% of the total score, representing the most informative attributes for clustering seismic data. This selection, from an original pool of 63 attributes, ensures reduced dimensionality while preserving interpretive accuracy for the detection of salt dome geobodies.

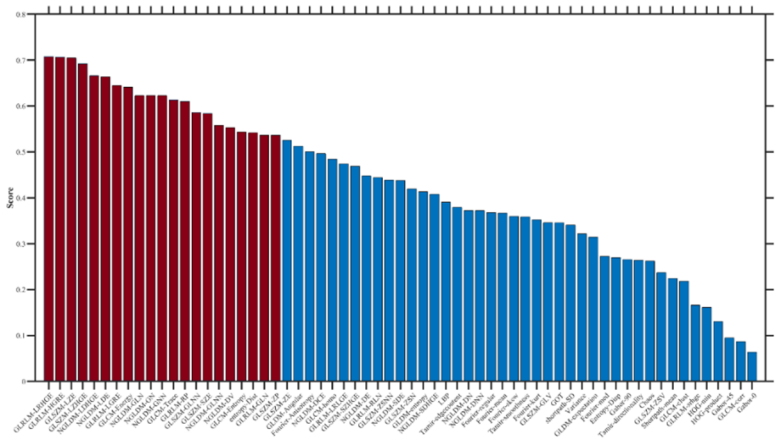

Figure 4. Scoring of attributes using the Laplacian method, red columns are selected for clustering.

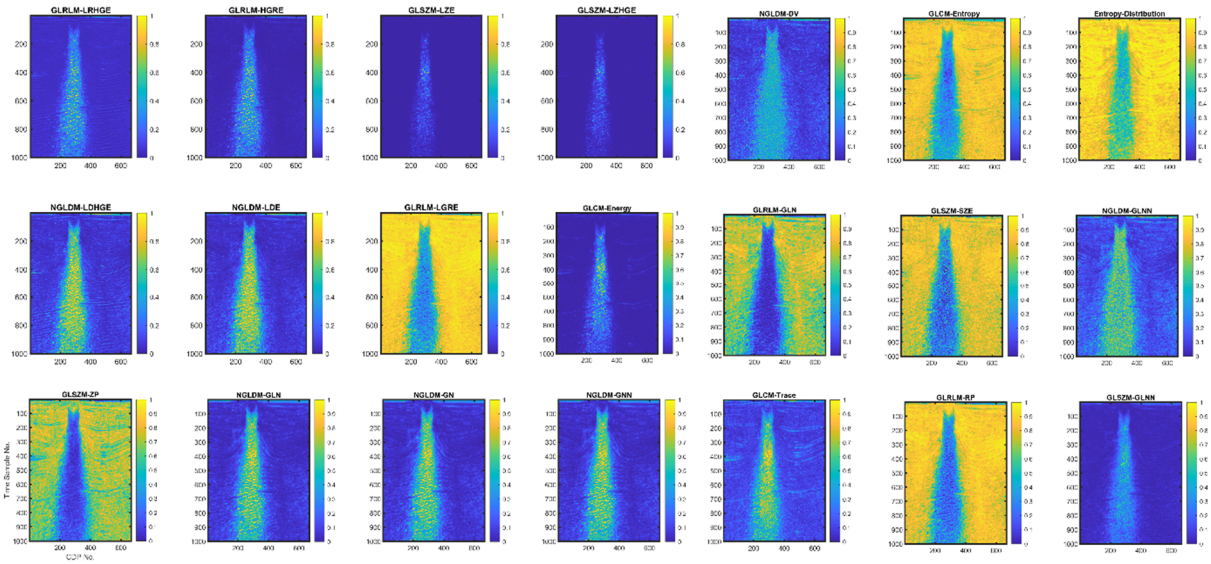

Figure 5. The 21 selected attributes through attribute selection algorithm from the 63 attributes listed in Table 1; It is notable that these attributes are shown after rescaling.

2.5. Clustering

Clustering is one of the most important and widely used unsupervised learning methods, aiming to partition a dataset into groups such that members within each group are highly similar to each other and distinctly different from members of other groups. This process helps uncover hidden structures in data and facilitates subsequent analysis. Various similarity measures exist, with Euclidean distance being among the most commonly used [1].

The K-Means algorithm, as one of the simplest and most popular clustering methods, begins by randomly selecting K initial centers $\{m_1, m_2, \dots, m_K\}$. Each data point $x_i \in \mathbb{R}^D$ is then assigned to the nearest center. After assignment, cluster centers are updated as the mean of the points assigned to each cluster. This

iterative process continues until the cluster centers stabilize or a convergence criterion is met.

Given the limitations of classical algorithms, transforming the clustering problem into an optimization task and employing metaheuristic algorithms has proven effective for improving clustering quality. The objective is to find cluster centers that minimize the DB index (see Appendix B):

$$\min_{K,S,d} \frac{1}{K}\sum_{i=1}^{K} \max_{j\neq i}\left(\frac{S_{i,q}+S_{j,q}}{d_{i,j,t}}\right) \quad (3)$$

In this study, two well-known metaheuristic algorithms—Genetic Algorithm (GA) and Particle Swarm Optimization (PSO)—are utilized to solve the clustering problem.

The Genetic Algorithm is inspired by the natural evolution process and maintains a population of candidate solutions (chromosomes), each representing a set of cluster centers. Each chromosome is defined as a vector containing the coordinates of the K cluster centers in the D-dimensional feature space:

$$\text{Chromosome} = [m_1, m_2, \dots, m_K], m_j \in \mathbb{R}^D. \quad (4)$$

In each generation, data points are assigned to clusters based on the centers encoded in each chromosome, and the Davies-Bouldin index is calculated for each chromosome. The DB value is considered inversely proportional to the fitness function:

$$Fitness = \frac{1}{DB}. \quad (5)$$

The evolutionary process includes selection, crossover, and mutation operators:

- Selection: Superior chromosomes are selected using methods such as roulette wheel or tournament selection to have a higher chance of producing offspring.
- Crossover: Two parent chromosomes exchange parts of their genes (cluster centers) to produce new offspring. For example, single-point crossover is defined as:

$$\text{Child}_1 = [m_1^{(P1)}, \dots, m_c^{(P1)}, m_{c+1}^{(P2)}, \dots, m_K^{(P2)}],$$
$$\text{Child}_2 = [m_1^{(P2)}, \dots, m_c^{(P2)}, m_{c+1}^{(P1)}, \dots, m_K^{(P1)}] \quad (6)$$

where c is the crossover point and $P1, P2$ are the parents.

- Mutation: With a small probability, some genes (cluster center coordinates) are randomly altered to maintain population diversity and increase the chance of escaping local optima. Mutation is often implemented by adding Gaussian noise to the coordinates:

$$m_j' = m_j + \mathcal{N}(0, \sigma^2), \quad (7)$$

where $\mathcal{N}(0, \sigma^2)$ is Gaussian noise with zero mean and variance σ^2.

This process repeats until a stopping criterion such as a maximum number of generations or lack of improvement in fitness is met. This structure enables GA to extensively explore the search space and avoid premature convergence, making it an effective method for improving clustering quality compared to classical algorithms [22].

Particle Swarm Optimization (PSO) is inspired by social behaviors observed in groups such as bird flocks. Each particle represents a candidate solution (cluster centers) moving in the search space. Particles update their velocity and position based on their personal best position and the global best position found by the swarm. The velocity and position update equations are:

$$v_i(t+1) = w \cdot v_i(t) + c_1 \cdot r_1 \cdot \left(p_i^{best} - x_i(t)\right) + c_2 \cdot r_2 \cdot \left(g^{best} - x_i(t)\right), x_i(t+1) = x_i(t) + v_i(t+1), \quad (8)$$

Where, w is the inertia weight balancing global and local search, c_1 and c_2 are the cognitive and social learning coefficients, r_1 and r_2 are random numbers uniformly distributed in [40].

Numerous studies have shown that PSO, due to its simple structure, faster convergence speed, and fewer parameters, performs very well in continuous optimization problems and is often computationally more efficient than GA. However, PSO may get trapped in local optima, which can be mitigated by proper parameter tuning or hybridization with other methods. Conversely, GA, though slower to converge,

provides better exploration capabilities and robustness against local optima. Employing metaheuristic algorithms such as GA and PSO in clustering, especially for high-dimensional and complex datasets, offers a powerful approach to overcome the limitations of classical methods and achieve higher-quality clustering results. Throughout this study, the Davies-Bouldin index serves as the primary metric for quantitatively comparing the performance of different clustering algorithms.

3. Result

The objective of this study is to identify the salt dome geobody by clustering seismic attributes, thereby facilitating automatic interpretation of seismic data. To achieve this, superpixels were generated, and effective attributes were selected based on the Laplacian score. For each superpixel, an attribute vector was computed according to the selected attributes. The clustering of superpixels was then performed using both classical and metaheuristic K-Means methods, with the results shown in Figure 6. Figure 6(a) illustrates the clustering results using the classical K-Means method with two user-defined clusters. It was observed that, in the automatic identification of reflection patterns based on seismic attributes, the clusters tend to be non-spherical and do not exhibit clear separability in the attribute space. Consequently, the classical K-Means method yielded suboptimal results, as illustrated in Figure 6(a). In contrast, Figures 6(b) and 6(c) display clustering results using metaheuristic optimization algorithms, specifically Genetic Algorithm (GA) and Particle Swarm Optimization (PSO). The parameter values used for each optimization algorithm are provided in Table 2.

These metaheuristic methods yielded more coherent results in distinguishing the salt dome from the surrounding stratified layers, demonstrating improved identification of the salt dome geobody. A comprehensive comparison of the employed methods and an evaluation of the results against actual geological data will be presented in the discussion section. The initial findings indicate that metaheuristic clustering algorithms significantly enhance the accuracy and reliability of automatic seismic interpretation for salt dome detection.

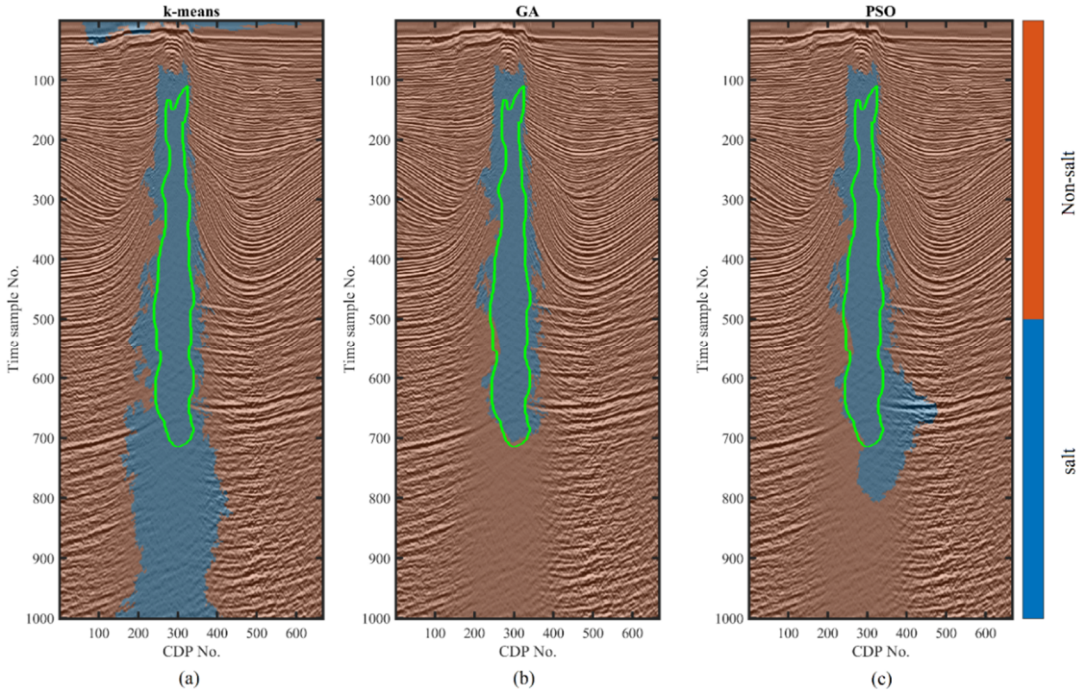

Figure 6. Automatic reflection pattern identification using clustering seismic attributes: (a) k-means, (b) GA and (c) PSO. The green line is the interpreted boundary of the salt dome resulting from the average manual interpretation of three professional interpreters.

Table2. Parameter related to two Metaheuristic methods

Method	Parameter								
	Population size	Maximum iteration	Crossover percentage	Mutation percentage	Mutation rate	Inertia weight	Damping ratio	Personal learning coefficient	Global learning coefficient
GA	500	1000	0.8	0.3	0.02	----	----	----	----
PSO	500	1000	----	----	----	0.7298	1	1.4962	1.4962

4. Discussion

In this study, to quantitatively evaluate the accuracy of salt dome geobody identification, an unsupervised clustering method based on metaheuristic optimization was employed. The validity of the results obtained from this method was assessed by comparing them with manual interpretations performed by three expert interpreters; the interpreted areas by these experts are indicated by green lines in Figure 2a. The quantitative comparison results are presented in Table 2.

To assess the identification accuracy of the salt dome, the extracted results were first binarized into two classes: "salt" and "non-salt." This binarization enabled the application of quantitative evaluation metrics. The F1-score was used as the primary evaluation metric, which combines precision and recall, and is especially valuable when dealing with imbalanced datasets. The F1-score is defined as follows:

$$\mathrm{F1-Score} = 2 \times \frac{\mathrm{precision} \times \mathrm{recall}}{\mathrm{precision} + \mathrm{recall}}$$

$$\mathrm{precision} = \frac{TP}{TP + FP} \qquad (9)$$

$$\mathrm{recall} = \frac{TP}{TP + FN}$$

where, the values of TP (True Positive), FP (False Positive), FN (False Negative), and TN (True Negative) are obtained from the classification confusion matrix. The F1 score ranges from 0 (worst) to 1 (best), and it's especially useful when both false positives and false negatives matter [10]. The F1-score values for the binarized clustering results in this study are presented in Table 3. The results demonstrate that metaheuristic algorithms provide outputs that are closer and more consistent with manual interpretation compared to classical methods. Notably, the genetic algorithm has significantly outperformed others by accurately delineating the salt dome geobody from the surrounding sediments.

Table 3. Comparison of the accuracy and F1-score of results.

attribute	F1_score	accuracy
K-means	80.61	83.86
GA	83.08	95.70
PSO	82.48	92.94

These findings highlight the effectiveness of metaheuristic optimization methods for seismic data analysis and the precise identification of complex geological structures, suggesting their potential as effective tools in geological studies and natural resource exploration. From a geological perspective, the improved delineation of salt dome boundaries achieved through the proposed metaheuristic clustering approach has direct implications for hydrocarbon exploration. The identified salt dome geometries reveal distinct deformation patterns and boundary contrasts that likely correspond to structural uplifts and potential hydrocarbon traps. In particular, the sharp lateral terminations observed in the clustered results may indicate sealing surfaces along the flanks of the dome, which represent favorable sites for hydrocarbon accumulation. Moreover, the strong correspondence between automatically detected salt boundaries and expert interpretations confirms the reliability of the method for predicting reservoir geometry and assessing

drilling risks. Overall, these results demonstrate that beyond algorithmic performance, the proposed workflow provides meaningful geological insights into subsurface salt-related structures and enhances their interpretation in the context of real-world reservoir characterization.

To evaluate the quality of clustering obtained from different methods, the Davies-Bouldin Index was used as a well-established and reliable metric. This index simultaneously measures the internal cohesion of each cluster and the separation between clusters, providing a comprehensive assessment of the clustering algorithm's performance. A lower Davies-Bouldin Index value indicates higher clustering quality and better separation between clusters.

The results showed that both metaheuristic algorithms, Genetic Algorithm (GA) and Particle Swarm Optimization (PSO), performed better than classical methods. Specifically, the Davies-Bouldin Index values were 18.9802 for GA and 26.1813 for PSO, while classical methods yielded a value of 31.7854. This indicates that the clustering quality obtained by the Genetic Algorithm is superior.

As shown in Table 4, the Genetic Algorithm achieves the highest accuracy and the lowest DB index, indicating superior clustering quality compared to the other methods. Figure 7 illustrates the changes in the optimal cost (objective function value) over the number of iterations for the GA and PSO algorithms. As observed, PSO converges faster than GA and reduces the cost more steeply in the initial iterations, demonstrating PSO's higher efficiency in reaching near-optimal solutions quickly.

However, although PSO converges earlier, the final optimal cost and Davies-Bouldin Index values are lower (better) for the GA algorithm. This suggests that despite its slower convergence rate, the Genetic Algorithm has a better capability to find more optimal solutions and produce higher-quality clustering.

Beyond the algorithmic advantages, the proposed metaheuristic clustering framework also provides new geological insights into salt tectonics. The identified dome boundaries and deformation fronts correlate well with structural highs and closure zones that typically act as hydrocarbon traps. Furthermore, the sharp textural contrasts at the dome margins may indicate overthrust or fault-assisted migration pathways. Such insights can support field development strategies, particularly for well placement and risk management in drilling through over-pressured zones adjacent to salt bodies.

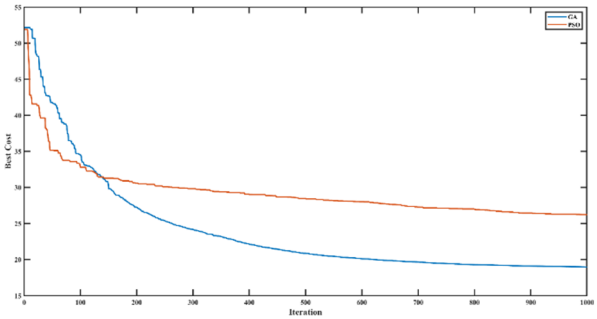

Figure 7. Best cost diagram based on iteration for GA, PSO and ROA algorithm.

Table 4. Results of DB index based on GA, PSO and k-means algorithm.

Method	GA	PSO	Classic
DB index	18.9802	26.1813	31.7854

5. Conclusions

In this study, we proposed a novel unsupervised framework for the automatic identification of salt dome geobodies in 2D seismic sections by leveraging clustering techniques based on metaheuristic optimization algorithms. The methodology integrated a comprehensive suite of both conventional and advanced textural seismic attributes, followed by attribute selection using the Laplacian Score to enhance model efficiency and interpretability. The selected attributes were then clustered using metaheuristic-based algorithms, which are capable of dynamically determining the optimal number of clusters and effectively handling complex, non-spherical data distributions.

The proposed approach was validated on real seismic data from an oil field in southwest Iran and benchmarked against manual interpretations provided by multiple expert interpreters. The results demonstrated that the metaheuristic-based clustering method not only improved the accuracy and robustness of salt dome delineation but also significantly reduced interpreter bias and the time required for analysis. Furthermore, the use of the Davies-Bouldin index as a clustering

quality metric confirmed that the metaheuristic algorithms outperformed traditional clustering techniques such as k-means, especially in scenarios involving complex geological structures.

Despite these promising outcomes, some limitations remain. The current study was conducted on a single 2D seismic section, and the scalability of the method to larger and more diverse 3D datasets remains to be explored. Additionally, while the proposed framework reduces dependency on labeled data, its performance is still sensitive to the selection of input attributes and algorithmic parameters.

Future research will focus on optimizing the computational efficiency of the algorithm to enable large-scale 3D seismic data analysis. The method will also be tested and validated across multiple datasets from various geological settings to ensure its robustness and general applicability. Integrating supplementary data sources, such as petrophysical and well-log information, could further enhance the interpretational power and reliability of the automated workflow. Ultimately, this research paves the way for the development of high-performance, fully automated tools for seismic data analysis and interpretation, supporting more efficient and objective subsurface characterization in the oil and gas industry. The presented unsupervised metaheuristic clustering framework not only advances automated seismic interpretation but also offers a practical and scalable tool for reducing interpreter bias in subsurface characterization and hydrocarbon exploration.

Appendix

A. Laplacian Score

For a given attribute $\boldsymbol{a}^j = \left[a_1^j, a_2^j, \cdots, a_m^j\right]^T$ with a_i^j representing the value of the j-th attribute for the i-th sample, the full dataset consists of i-th sample such samples across n attributes. [26].

A nearest-neighbor graph is formed, connecting each node to its local neighbors. The strength of the connection between two samples $\boldsymbol{x}_i$and $\boldsymbol{x}_j$ is measured using a Gaussian kernel as:

$$s_{ij} = e^{\frac{\|\boldsymbol{x}_i - \boldsymbol{x}_j\|^2}{t}}, \quad \text{(A1)}$$

where t is a scaling parameter determined either heuristically or through subsampling methods that explore different values and assess structural consistency. All similarity values are assembled into a matrix $\mathbf{S} = \left[s_{ij}\right]$, where unconnected nodes yield zero entries. A diagonal matrix **D** captures the sum of similarities for each sample (i.e., node degree), and the graph Laplacian is defined **L** as:

$$\begin{aligned} &L = D - S, \\ &D = diag(S \times o). \end{aligned} \quad \text{(A2)}$$

Here, $\boldsymbol{o}$ is a column vector of ones. Each attribute's relevance is evaluated using: [26]:

$$\begin{aligned} &l_j = \frac{k_j^T L k_j}{k_j^T D k_j} = 1 - \frac{k_j^T S k_j}{k_j^T D k_j}, \\ &k_j = a_j - \frac{a_j^T D o}{o^T D o} \times o. \end{aligned} \quad \text{(A3)}$$

In MATLAB implementations, the quantity $\boldsymbol{k_j^T S k_j / k_j^T D k_j}$ is used directly to rank attributes, with higher values indicating greater importance. This is a slight deviation from the original Laplacian score definition, where lower scores signify higher relevance.

B. K-Means clustering as optimization problem

The primary objective of K-Means is to minimize the sum of squared errors (SSE), defined as [3]:

$$SSE = \sum_{k=1}^{K} \sum_{x_i \in c_k} \|x_i - c_k\|^2, c_k = \frac{1}{|c_k|} \sum_{x_i \in c_k} x_i. \quad \text{(B1)}$$

Despite its simplicity and computational efficiency, K-Means suffers from limitations such as sensitivity to the initial cluster centers and the tendency to get trapped in local optima, which may degrade clustering quality.

To evaluate clustering quality, the Davies-Bouldin (DB) index is widely recognized as a reliable metric. This index measures the ratio of intra-cluster scatter to inter-cluster separation, aiming to minimize this ratio so that clusters are compact and well-separated. The DB index is computed as follows [14]:

$$S_{i,q} = \left(\frac{1}{n_i} \sum_{x \in c_i} d(x, m_i)^q \right)^{\frac{1}{q}}, d_{i,j,t} = \|m_i - m_j\|_t, \quad \text{(B2)}$$

$$DB = \frac{1}{K} \sum_{i=1}^{K} \max_{j \neq i} \left(\frac{S_{i,q} + S_{j,q}}{d_{i,j,t}} \right), \quad \text{(B3)}$$

where n_i is the number of points in cluster i, $d(x, m_i)$ is the Euclidean distance between point x and cluster center m_i, and parameters q and t are positive integers that can be chosen independently. Using the DB index, the K-Means clustering problem can be formulated as an optimization problem, in which the number of clusters and their centers are determined such that the DB index is minimized.

$$\min_{K,S,d} \frac{1}{K} \sum_{i=1}^{K} \max_{j \neq i} \left(\frac{S_{i,q} + S_{j,q}}{d_{i,j,t}} \right). \quad \text{(B4)}$$

Reference

[1]. Abualigah, L., Gandomi, A. H., Elaziz, M. A., Hamad, H. A., Omari, M., Alshinwan, M., & Khasawneh, A. M. (2021). Advances in meta-heuristic optimization algorithms in big data text clustering. *Electronics*, *10*(2), 101.

[2]. Achanta, R., Shaji, A., Smith, K., Lucchi, A., Fua, P., & Süsstrunk, S. (2012). SLIC superpixels compared to state-of-the-art superpixel methods. *IEEE transactions on pattern analysis and machine intelligence*, *34*(11), 2274-2282.

[3]. Aggarwal, C. C., & Reddy, C. K. (2014). *Data clustering*. CRC Press, Londra.

[4]. Amin, A., & Deriche, M. (2016). Salt-dome detection using a codebook-based learning model. *IEEE Geoscience and Remote Sensing Letters*, *13*(11), 1636-1640.

[5]. Amin, A., Deriche, M., Shafiq, M. A., Wang, Z., & AlRegib, G. (2017). Automated salt-dome detection using an attribute ranking framework with a dictionary-based classifier. *Interpretation*, *5*(3), SJ61-SJ79.

[6]. Azami, H., da Silva, L. E. V., Omoto, A. C. M., & Humeau-Heurtier, A. (2019). Two-dimensional dispersion entropy: An information-theoretic method for irregularity analysis of images. *Signal Processing: Image Communication*, *75*, 178-187.

[7]. Azami, H., Escudero, J., & Humeau-Heurtier, A. (2017). Bidimensional distribution entropy to analyze the irregularity of small-sized textures. *IEEE Signal Processing Letters*, *24*(9), 1338-1342.

[8]. Berthelot, A., Solberg, A. H., & Gelius, L.-J. (2013). Texture attributes for detection of salt. *Journal of Applied Geophysics*, *88*, 52-69.

[9]. Celecia, A., Figueiredo, K., Rodriguez, C., Vellasco, M., Maldonado, E., Silva, M. A., Rodrigues, A., Nascimento, R., & Ourofino, C. (2021). Unsupervised Machine Learning Applied to Seismic Interpretation: Towards an Unsupervised Automated Interpretation Tool. *Sensors*, *21*(19), 6347.

[10]. Chicco, D., & Jurman, G. (2020). The advantages of the Matthews correlation coefficient (MCC) over F1 score and accuracy in binary classification evaluation. *BMC genomics*, *21*, 1-13.

[11]. Chopra, S., & Marfurt, K. J. (2005). Seismic attributes—A historical perspective. *Geophysics*, *70*(5), 3SO-28SO.

[12]. Chopra, S., & Marfurt, K. J. (2007). *Seismic attributes for prospect identification and reservoir characterization*. SEG Publisher.

[13]. Cohen, I., Coult, N., & Vassiliou, A. A. (2006). Detection and extraction of fault surfaces in 3D seismic data. *Geophysics*, *71*(4), P21-P27.

[14]. Davies, D. L., & Bouldin, D. W. (1979). A cluster separation measure. *IEEE transactions on pattern analysis and machine intelligence*(2), 224-227.

[15]. Di, H., & Gao, D. (2017). Nonlinear gray-level co-occurrence matrix texture analysis for improved seismic facies interpretation. *Interpretation*, *5*(3), SJ31-SJ40.

[16]. Di, H., Gao, D., & AlRegib, G. (2019). Developing a seismic texture analysis neural network for machine-aided seismic pattern recognition and classification. *Geophysical Journal International*, *218*(2), 1262-1275.

[17]. Di, H., Wang, Z., & AlRegib, G. (2018). *Seismic fault detection from post-stack amplitude by convolutional neural networks* 80th EAGE Conference and Exhibition 2018.,

[18]. Efe, O., & Ozakin, A. (2024). The seismic purifier: An unsupervised approach to seismic signal detection via representation learning. *arXiv preprint arXiv:2407.18402*.

[19]. Eichkitz, C. G., Amtmann, J., & Schreilechner, M. G. (2013). Calculation of grey level co-occurrence matrix-based seismic attributes in three dimensions. *Computers & Geosciences*, *60*, 176-183.

[20]. Farrokhnia, F., RoshandelKahoo, A., & Soleimani, M. (2018). Automatic salt dome detection in seismic data by combination of attribute analysis on CRS images and IGU map delineation. *Journal of Applied Geophysics*, *159*, 395-407.

[21]Frutuoso, R. L., Gomes, J. P. P., dos Santos, E. M., Cavalcante-Neto, J. B., & Vidal, C. A. (2016). Texture Analysis using Informed Search in Graphs. 2016 29th SIBGRAPI Conference on Graphics, Patterns and Images (SIBGRAPI),

[22]. Ghezelbash, R., Maghsoudi, A., & Carranza, E. J. M. (2020). Optimization of geochemical anomaly detection using a novel genetic K-means clustering (GKMC) algorithm. *Computers & Geosciences*, *134*, 104335.

[23]. Gray, F. D., Anderson, P. F., & Gunderson, J. A. (2006). Prediction of shale plugs between wells in heavy oil sands using seismic attributes. *Natural Resources Research*, *15*(2), 103-109.

[24]. Halpert, A. D., Clapp, R. G., & Biondi, B. (2014). Salt delineation via interpreter-guided 3D seismic image segmentation. *Interpretation*, *2*(2), T79-T88.

[25]. Haralick, R. M., Shanmugam, K., & Dinstein, I. H. (2007). Textural features for image classification. *IEEE Transactions on systems, man, and cybernetics*(6), 610-621.

[26]He, X., Cai, D., & Niyogi, P. (2005). Laplacian score for feature selection. Advances in neural information processing systems, Vancouver, British Columbia, Canada.

[27]Hegazy, T., & AlRegib, G. (2014). Texture attributes for detecting salt bodies in seismic data. SEG Technical Program Expanded Abstracts 2014,

[28]. Herron, D. A. (2011). *First steps in seismic interpretation*. Society of Exploration Geophysicists.

[29]. Hosseini-Fard, E., Roshandel-Kahoo, A., Soleimani-Monfared, M., Khayer, K., & Ahmadi-Fard, A. R. (2022). Automatic seismic image segmentation by introducing a novel strategy in histogram of oriented gradients. *Journal of Petroleum Science and Engineering*, *209*, 109971.

[30]. Hu, Z., Zou, Q., & Li, Q. (2015). Watershed superpixel. 2015 IEEE International Conference on Image Processing (ICIP),

[31]. Humeau-Heurtier, A. (2019). Texture feature extraction methods: A survey. *IEEE access*, *7*, 8975-9000.

[32]. Junior, J. J. d. M. S., Backes, A. R., & Cortez, P. C. (2013). Texture analysis and classification using shortest paths in graphs. *Pattern Recognition Letters*, *34*(11), 1314-1319.

[33]. Khayer, K., Roshandel-Kahoo, A., Soleimani-Monfared, M., & Kavoosi, K. (2022). Combination of seismic attributes using graph-based methods to identify the salt dome boundary. *Journal of Petroleum Science and Engineering*, *215*, 110625.

[34]. Khayer, K., Roshandel Kahoo, A., Soleimani Monfared, M., Tokhmechi, B., & Kavousi, K. (2022). Target-Oriented fusion of attributes in data level for salt dome geobody delineation in seismic data. *Natural Resources Research*, *31*(5), 2461-2481.

[35]. Larsen, E., Purves, S., Economou, D., & Alaei, B. (2018). Is machine learning taking productivity in petroleum geoscience on a Moore's Law trajectory? *First break*, *36*(12), 135-141.

[36]. Lei, T., Jia, X., Liu, T., Liu, S., Meng, H., & Nandi, A. K. (2019). Adaptive morphological reconstruction for seeded image segmentation. *IEEE transactions on image processing*, *28*(11), 5510-5523.

[37]. Lin, J. (1991). Divergence measures based on the Shannon entropy. *IEEE Transactions on Information Theory*, *37*(1), 145-151.

[38]. Liu, B., Yasin, Q., Sohail, G. M., Chen, G., Ismail, A., Ma, Y., & Fu, X. (2023). Seismic characterization of fault and fractures in deep buried carbonate reservoirs using CNN-LSTM based deep neural networks. *Geoenergy Science and Engineering*, *229*, 212126.

[39]. Liu, N., Zhang, Z., Zhang, H., Wang, Z., Gao, J., Liu, R., & Zhang, N. (2024). Multiple-frequency attribute blending via adaptive uniform manifold approximation and projection and its application on hydrocarbon reservoir delineation. *Geophysics*, *89*(1), WA195-WA206.

[40]. Luu, K., Noble, M., Gesret, A., Belayouni, N., & Roux, P.-F. (2018). A parallel competitive Particle Swarm Optimization for non-linear first arrival traveltime tomography and uncertainty quantification. *Computers & Geosciences*, *113*, 81-93.

[41]. Maani, R., Kalra, S., & Yang, Y.-H. (2013). Noise robust rotation invariant features for texture classification. *Pattern recognition*, *46*(8), 2103-2116.

[42].Mammadov, O., Shafiyev, A., Malikov, R., Asgarov, H., Karimli, J., Shahsenov, I., Yeleskina, T., Karimli, I., & Abdullayev, N. (2023). Seismic Facies Clustering via Spectral Decomposition using Machine Learning. SPE Caspian Technical Conference and Exhibition,

[43]. Meldahl, P., Heggland, R., Bril, B., & de Groot, P. (2001). Identifying faults and gas chimneys using multiattributes and neural networks. *The leading edge*, *20*(5), 474-482.

[44]. Naseer, M. T. (2024). Seismic Attributes and Inverse Quantitative Static Density–Porosity–Constraint Reservoir Simulations of Naturally-Fractured Hydrocarbon-Bearing Lower Cretaceous Shallow-Marine Architectures, Onshore Indus, Pakistan. *Natural Resources Research*, *33*(1), 213-238.

[45]. Roberts, A. (2001). Curvature attributes and their application to 3 D interpreted horizons. *First break*, *19*(2), 85-100.

[46]. Roshandel Kahoo, A., Soleimani Monfared, M., & Radad, M. (2021). Identification and modeling of salt dome in seismic data using three-dimensional texture gradient. *Iranian Journal of Geophysics*, *15*(1), 19-33.

[47]. Sain, K., & Kumar, P. C. (2022). *Meta-attributes and artificial networking: A new tool for seismic interpretation*. John Wiley & Sons.

[48]. Sarma, R., & Gupta, Y. K. (2021). *A comparative study of new and existing segmentation techniques* IOP conference series: materials science and engineering,

[49]. Seydoux, L., Steinmann, R., Mouaoued, S., Esfahani, R., & Campillo, M. (2024). *Revealing and interpreting patterns from continuous seismic data with unsupervised learning*.

[50]. Shafiq, M. A., Alshawi, T., Long, Z., & AlRegib, G. (2016). Salsi: A new seismic attribute for salt dome detection. 2016 IEEE International Conference on Acoustics, Speech and Signal Processing (ICASSP),

[51]. Silva, L. E. V., Senra Filho, A., Fazan, V. P. S., Felipe, J. C., & Junior, L. M. (2016). Two-dimensional sample entropy: Assessing image texture through irregularity. *Biomedical Physics & Engineering Express*, *2*(4), 045002.

[52]Solberg, A., Berthelot, A., & Gelius, L. (2011). Gabor filters for segmentation of salt structures. 73rd EAGE Conference and Exhibition incorporating SPE EUROPEC 2011,

[53]. Soltani, P., Kahoo, A. R., & Hasanpour, H. (2023). Proposing new seismic texture attributes based on novel gray level matrix with application to salt dome detection. *Journal of Applied Geophysics*, *218*, 105214.

[54]. Soltani, P., Kahoo, A. R., & Hasanpour, H. (2025). Automatic identification and separation of reflection patterns with the help of clustering of seismic attributes in a Rain optimization meta-heuristic algorithm. *Journal of Applied Geophysics*, 105690.

[55]. Waldeland, A. U., Jensen, A. C., Gelius, L.-J., & Solberg, A. H. S. (2018). Convolutional neural networks for automated seismic interpretation. *The leading edge*, *37*(7), 529-537.

[56]. Wang, Q., Wang, Z., Gao, D., Gao, Z., Jia, J., Zhu, J., & Gao, J. (2024). Seismic attribute analysis with a combination of convolutional autoencoder and random forest in a turbidite reservoir. *Geophysics*, *89*(1), WA207-WA217.

[57]. Yang, J., Lu, R., Tao, W., Cai, M., Liu, G., & Sun, X. (2024). MultiURNet for 3D seismic fault attributes fusion detection combined with PCA. *Journal of Applied Geophysics*, *221*, 105296.

[58]. Zhang, J., Liang, J., Zhang, C., & Zhao, H. (2015). Scale invariant texture representation based on frequency decomposition and gradient orientation. *Pattern Recognition Letters*, *51*, 57-62.

[59]. Zhang, Z., Liu, N., Liu, R., Lu, M., Wei, T., & Gao, J. (2024). Adaptive Multi-frequency Attribute Analysis and its Application on Reservoir Characterization. *IEEE Transactions on geoscience and remote sensing*.

[60]. Zhao, T. (2018). Seismic facies classification using different deep convolutional neural networks. SEG International Exposition and Annual Meeting,